Published in Proceedings of the 2004 ASME Wind Energy Symposium, Paper No. AIAA-2004-0502, pp. 151-161, Reno, Nevada, January 2004.

AIAA-2004-0502

A COMPARISON OF WIND TURBINE DESIGN LOADS IN DIFFERENT ENVIRONMENTS USING INVERSE RELIABILITY

Korn Saranyasoontorn
Lance Manuel
Department of Civil Engineering, University of Texas at Austin, Austin, TX 78712

ABSTRACT

The influence of turbulence conditions on the design loads for wind turbines is investigated by using inverse reliability techniques. Alternative modeling assumptions for randomness in the gross wind environment and in the extreme response given wind conditions to establish nominal design loads are studied. Accuracy in design load predictions based on use of the inverse first-order reliability method (that assumes a linearized limit state surface) is also investigated. An example is presented where three alternative nominal load definitions are used to estimate extreme flapwise (out-of-plane) bending loads at a blade root for a 600kW three-bladed horizontal-axis wind turbine located at onshore and offshore sites that were assumed to experience the same mean wind speed but different turbulence intensities. It is found that second-order (curvature-type) corrections to the linearized limit state function assumption inherent in the inverse first-order reliability approach are insignificant. Thus, we suggest that the inverse first-order reliability method is an efficient and accurate technique of predicting extreme loads. Design loads derived from a full random characterization of wind conditions as well as short-term maximum response (given wind conditions) may be approximated reasonably well by simpler models that include only the randomness in the wind environment but account for response variability by employing appropriately derived "higher-than-median" fractiles of the extreme bending loads conditional on specified inflow parameters. In the various results discussed, it is found that the higher relative turbulence at the onshore site leads to larger blade bending design loads there than at the offshore site. Also, for both onshore and offshore environments accounting for response variability is found to be slightly more important at longer return periods (i.e., safer designs).

INTRODUCTION

In codified reliability-based design (e.g., in the conventional load-and-resistance-factor-design or LRFD procedure), one typically uses a design checking equation to describe what is required for safety against a specified limit state and to guarantee a specified reliability (or probability of failure). Such a design checking equation involves scaling of a nominal resistance or capacity by a resistance factor and the simultaneous scaling of a nominal load by a separate load factor. The nominal load, L_{nom}, is typically defined as a "load" or environmental input associated with a certain return period – e.g., a 50-year return period wind speed. For wind turbine generator systems, a similar reliability-based design format is employed in the IEC 61400-1 guidelines where the load and resistance factors are combined into a single factor that represents a safety factor for "consequences of failure" (see IEC/TC88 61400-1 ed. 2, 1998).

Various alternative definitions of the nominal load level may be employed to account for load variability. We discuss a few such definitions here that essentially differ in the degree to which uncertainties in the inflow and response are represented. The key uncertainties in the design of wind turbines arise from (i) the gross inflow parameters, usually taken to be the ten-minute mean horizontal wind speed at hub height and the standard deviation (or, alternatively, turbulence intensity) of the same wind speed process; and (ii) the ten-minute maximum load/response conditional on the inflow parameters.

In the following, we refer to the inflow parameters as simply mean and standard deviation of wind speed, with an understanding that we are referring to statistics of the time-varying horizontal wind speed process at hub height. We consider an extreme flapwise (out-of-plane) bending moment at the blade root as the load of interest. Our objective is to establish appropriate nominal design loads for several target reliability levels (or, equivalently, for several different return periods). These loads defined with different degrees of

complexity in the assumptions on the variability of the key random variables are then compared.

Because offshore wind turbines are of much interest lately, we choose to discuss how design loads (for safety against failure in ultimate limit states) for a specific 600 kW three-bladed horizontal-axis wind turbine, might differ in two distinct environments – one onshore, the other offshore. We will focus on only one of the several differences in environment conditions between onshore and offshore sites – namely, the lower turbulence levels experienced offshore relative to onshore sites. In the following, we discuss how the inverse reliability approach proposed here may be applied in each of these sites. For the sake of simplicity, we omit characterization of the wave loading randomness at the offshore site and we also assume that the wind speed at both sites is of the same magnitude and described by the same probability distribution. In reality, typical offshore sites will have higher mean wind speeds than onshore sites and will require consideration of randomness in wave loading, tides, water depth, etc. The present study intentionally only includes two random variables to describe the environment. It will become clear in the following that the inclusion of environmental parameters (e.g., significant wave height at the offshore site) beyond the mean and standard deviation of the ten-minute wind speed at hub height only implies increasing the dimensions of the space of the geometrically described inverse reliability procedure outlined here.

INVERSE RELIABILITY PROCEDURES

Inverse reliability techniques are commonly used when there is interest in establishing design levels associated with a specified reliability of probability of failure. A heuristically appealing Inverse First-Order Reliability Method (Inverse FORM) proposed by Winterstein *et al*. (1993) is one such example of an inverse reliability technique that has been applied to estimate design loads in many applications including earthquake engineering (Li and Foschi, 1998), offshore structures (Winterstein *et al*., 1993), and more recently wind turbines (Fitzwater *et al*., 2003; Saranyasoontorn and Manuel, 2003). In one variation of this approach, termed the "environmental contour" approach, the environmental random variables are uncoupled from the structural response. Then, the procedure considers, as in conventional "forward-FORM" analyses, that the governing limit state function may be linearized locally near the "design point" and a search performed for the largest load resulting from all points on an environmental contour associated with the return period of interest. This approach is appealing in that it uncouples the environmental random variables from the structural response in the analysis. It will be referred to as the "2-D Model" in the following since it will essentially involve including complete probability information for only the two inflow/environmental random variables (mean and standard deviation of wind speed).

Two issues related to accuracy of design loads derived using the Inverse FORM are discussed next:

1. *Linearized limit state surface*: The Inverse FORM approach is an approximate procedure for deriving design loads since it uses a local linearized limit state function with which the desired probability of failure (or reliability) is associated. The true limit state function may be highly nonlinear near the design point where the linearizing is done. Thus, it is possible that large errors may result since the target reliability will be different if the true limit state function is employed.

2. *Response variability*: In order to uncouple environment variables from structural response, the 2-D model that will be discussed does not retain the complete probabilistic description of the response. It instead represents the response simply by using its "median" value conditional on the random inflow variables. This can lead to significant differences and compromises in accuracy relative to the 3-D model that includes a full description of response variability. We shall show that the 2-D model may still be used if fractile levels of the response other than the median are derived based on the use of omission sensitivity factors (Madsen, 1988) that account for variability in the response term. Saranyasoontorn and Manuel (2003) recommended a simple procedure using such omission sensitivity factors and local gradients of the limit state function to derive the appropriate fractile of the response that can lead to reasonably accurate design loads while retaining the advantages of the 2-D model (namely, that inflow and response are uncoupled).

In the numerical studies that follow, we address both of these issues and draw some general conclusions related to the extent to which they affect accuracy for the selected wind turbine in the onshore and offshore sites.

By way of background, it should be noted that Fitzwater *et al*. (2003) applied inverse reliability methods to study extreme loads on pitch- and stall-

regulated wind turbines where they employed results from aeroelastic simulations to represent the response given inflow conditions. The response variable there was treated as deterministic allowing the use of the 2-D environmental contour approach. In the present study, our interest is in estimating design extreme flapwise bending loads for a 600kW three-bladed horizontal-axis wind turbine that was previously studied by Ronold and Larsen (2000), where results from field measurements were reported and probabilistic models for response (loads) conditional on inflow conditions were presented. The distinction between the present study and that by Fitzwater *et al*. (2003) is that we propose alternative nominal load definitions (one of which includes response variability – the 3-D model) and we employ field data instead of simulations in developing parametric models for the random response conditional on inflow. Our alternative load definitions are based on what will be described as 1-D, 2-D, and 3-D models which refer to how the inflow and response variables are treated – i.e., whether deterministic or random. The full 3-D characterization of variables refers to modeling of all variables as random, while the other two models refer to simplifications where, in the 1-D case, only mean wind speed is modeled as random and, in the 2-D case, the mean and standard deviation of the wind speed are both modeled as random (but response is not).

Another recent study by Saranyasoontorn and Manuel (2003) used the Inverse FORM approach to estimate design extreme loads for the same turbine as in the present study. That study, however, includes a very detailed description of the differences between the 1-D, 2-D, and 3-D models which is omitted here. However, no detailed investigation of the assumption of linear limit state functions is provided in that study. Also, in the present study, onshore and offshore sites are compared; the earlier study focused on results for the onshore site alone.

The alternative nominal load definitions are presented next, along with a general background on the Inverse FORM framework for establishing design loads. Design load levels for three different return periods based on the alternative load models will be compared for the two sites where the 600kW wind turbine described by Ronold and Larsen (2000) will be assumed to be located.

ALTERNATIVE NOMINAL LOADS: A REVIEW

The use of Inverse FORM to establish nominal wind turbine loads with various degrees of modeling assumptions is briefly reviewed here. Greater detail related to these load definitions is included in Saranyasoontorn and Manuel (2003).

Our interest here is in obtaining estimates of a nominal load, L_{nom}, for failure in an extreme/ultimate limit state associated with bending of a wind turbine blade in its flapwise (out-of-plane) mode. We assume that the uncertainty in these extreme bending loads depends on inflow parameters and on short-term maximum loads conditional on the inflow parameters. As stated previously, the inflow parameters that characterize the wind are the ten-minute mean wind speed at hub height, U_{10}, and the standard deviation, σ, of the wind speed. The load, L_{nom}, considered here is the extreme flapwise bending moment at the root of a turbine blade corresponding to a specified return period of T years. From the field data on the wind turbine considered, ten-minute extremes of the random flapwise bending moment, BM_{ext}, are used to derive the nominal load, L_{nom}. For convenience, in discussions that follow, we will refer to the three short-term (i.e., ten-minute) random variables, U_{10}, σ, and BM_{ext} as X_1, X_2, and X_3 that make up the physical random variable space, $\boldsymbol{X}$.

Consider a situation where the joint probability description of X_1, X_2, and X_3 is available in the form of a marginal distribution for X_1 and conditional distributions for X_2 given X_1, and for X_3 given X_1 and X_2. The simplest definition of L_{nom} is based on a representative load derived from the T-year value of the random X_1 (mean wind speed) alone and consideration of X_2 (standard deviation on wind speed) and X_3 (ten-minute extreme bending load) only by representing these as conditional median values. In this model for L_{nom}, uncertainty is neglected in both X_2 and X_3. A second definition might be based on a representative T-year load that includes randomness in both X_1 and X_2 but still neglects uncertainty in the short-term load, X_3. Again, this load is held fixed at its median level given X_1 and X_2. Finally, a definition for nominal load could be based on the "true" T-year nominal load including uncertainty in all of the three variables. We refer to these definitions as "1-D", "2-D", and "3-D" probabilistic models respectively. Note that the load factor in the LRFD checking equation will be appropriately different for each of the nominal load definitions above in order to ensure that the design checking equation leads to consistent reliability estimates in each case.

It is possible to establish nominal loads by direct integration involving the conditional short-term maximum load distribution (given inflow conditions) and the joint density function of the inflow variables.

For the right choice of L_{nom}, integration will lead to the desired target probability of failure, P_f, as follows:

$$P_f = P[X_3 > L_{nom}] = \iint_{X_1,X_2} P[X_3 > L_{nom} \mid X_1, X_2] f_{X_1,X_2}(x_1, x_2) dx_1 dx_2 \quad (1)$$

where $f_{X_1,X_2}(x_1,x_2)$ is the joint probability density function of X_1 and X_2. Using Eq. (1) to obtain the nominal load would provide the "exact" load but would be computationally expensive to determine in practical situations. Also, not much would be learned about the inflow conditions that bring about this load. Inverse reliability procedures, on the other hand, are approximate but less computationally intensive and have an important advantage in that they offer useful insights into the derived load and about the associated inflow conditions. In particular, we will use the Inverse FORM approach proposed by Winterstein *et al*. (1993). An overview is presented next of how this method based on environmental contours works in the current study.

Consider a hypersphere of radius equal to the target reliability index, β, in an n-dimensional space describing independent standard normal variables, one for each of the physical random variables in the problem of interest. If at any point on this sphere, a tangent hyperplane were drawn, the probability of occurrence of points on the side of this hyperplane away from the origin is $\Phi(-\beta)$ based on a local linearization of the limit state function at the design point, where $\Phi(\ )$ refers to the Gaussian cumulative distribution function. Since each point on the sphere is associated with the same reliability level, if the nominal load desired is also for this same level, the points on the sphere can be systematically searched until the largest nominal load is obtained. Transformation from the standard normal ($\boldsymbol{U}$) space to the physical random variable ($\boldsymbol{X}$) space is necessary in order to obtain the nominal load. This is achieved by using the Rosenblatt transformation (Rosenblatt, 1952). In the present study, a complete probabilistic representation of the random variables requires that n is equal to 3. The selection of values of n equal to 1, 2, and 3 lead to different nominal loads, and can be explained geometrically. This has been done by Saranyasoontorn and Manuel (2003) in detail and is summarized in Table 1 which shows how the design load, X_3, may be determined if the various cumulative distribution functions, $F_{X_1}(x_1)$, $F_{X_2|X_1}(x_2)$, and $F_{X_3|X_1,X_2}(x_3)$, are known and a search is employed based on the auxiliary variable(s) and the target reliability index, β.

In summary, the 1-D model assumes that the ten-minute mean wind speed, X_1, is random but neglects the variability in the standard deviation of the wind speed, X_2, and in the ten-minute maximum response, X_3. In $\boldsymbol{U}$ space then, the n-dimensional "sphere" is a degenerate point, $u_1 = \beta$; $u_2 = u_3 = 0$. Similarly, the 2-D model assumes that only X_1 and X_2 are random; in $\boldsymbol{U}$ space, the n-dimensional "sphere" is a degenerate circle, $u_1^2 + u_2^2 = \beta^2$; $u_3 = 0$. The 3-D model treats all three variables as random and is represented by the 3-D sphere, $u_1^2 + u_2^2 + u_3^2 = \beta^2$. Because our target reliability is specified in terms of a return period (equal to T years) associated with the nominal load, L_{nom}, note that since X_3 is defined as the extreme value in ten minutes, we need to determine the appropriate value of β to be used in the Inverse-FORM approach described by the 1-D, 2-D, and 3-D models. This is done by setting $\beta = \Phi^{-1}(1-P_f)$ where β and P_f are related to the target return period (T years) and the number of ten-minute segments in T years. Assuming independence between extremes in the various ten-minute segments, for the three return periods studied here corresponding to 1, 20, and 50 years, the values of P_f are 1.90×10^{-5}, 9.51×10^{-7}, and 3.81×10^{-7}, respectively, and the values of β are 4.12, 4.76, and 4.95, respectively.

NUMERICAL STUDIES

The machine considered in this study is a 600kW stall-regulated horizontal-axis turbine with three 21.5-meter long rotor blades and a hub height of 44 meters. This turbine has been the subject of previous studies and is one for which field data as well as extrapolated design loads have been derived by Ronold and Larsen (2000). Probabilistic models for short-term maximum flapwise bending loads were also derived.

Here, the machine is assumed to be located at onshore and offshore sites with different turbulence conditions (i.e., different X_2 descriptions) but the same mean wind speed (X_1). The turbulence conditions used are based on recommendations of DNV/Risø (2002) for onshore and offshore environments. It should be noted that the standard deviation of X_2 (given X_1) referred to as $D[X_2|X_1]$, is almost the same in the onshore and offshore sites but the mean value (given X_1), referred to as $E[X_2|X_1]$, is significantly different as may be seen in Fig. 1. This implies that for the same mean wind speed assumed for the two sites, the wind turbine at the onshore site will experience greater turbulence than the one at the offshore environment.

Model	Variables needed in the Inverse-FORM procedure		
	U	Auxiliary Variables	***X***
1-D	$U_1 = \beta;\ U_2 = U_3 = 0$	None	$X_1 = F_{X_1}^{-1}\left[\Phi(\beta)\right]$ $X_2 = F_{X_2\|X_1}^{-1}\left[\Phi(0)\right]$ $X_3 = F_{X_3\|X_1,X_2}^{-1}\left[\Phi(0)\right]$
2-D	$U_1^2 + U_2^2 = \beta^2;\ U_3 = 0$	$\varphi;\ -\pi < \varphi \le \pi$	$X_1 = F_{X_1}^{-1}\left[\Phi(\beta\cos\varphi)\right]$ $X_2 = F_{X_2\|X_1}^{-1}\left[\Phi(\beta\sin\varphi)\right]$ $X_3 = F_{X_3\|X_1,X_2}^{-1}\left[\Phi(0)\right]$
3-D	$U_1^2 + U_2^2 + U_3^2 = \beta^2$	$\varphi,\theta;\ -\pi < \varphi \le \pi,\ 0 < \theta \le \pi$	$X_1 = F_{X_1}^{-1}\left[\Phi(\beta\cos\varphi\sin\theta)\right]$ $X_2 = F_{X_2\|X_1}^{-1}\left[\Phi(\beta\sin\varphi\sin\theta)\right]$ $X_3 = F_{X_3\|X_1,X_2}^{-1}\left[\Phi(\beta\cos\theta)\right]$

Table 1: Summary of Design Point Coordinates in *U* and *X* Space along with Auxiliary Variables needed in the Inverse FORM Procedure for the 1-D, 2-D, and 3-D Models, given a Target Reliability Index, β.

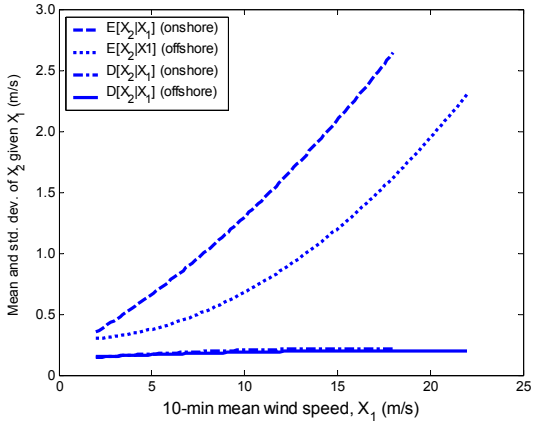

Figure 1: Conditional Mean and Standard Deviation of X_2 given the Ten-minute Mean Wind Speed, X_1.

The various probability distributions and parameters needed to model the inflow variables (X_1 and X_2) and the extreme flapwise bending moment (X_3) are summarized in Table 2. The inflow was modeled by assuming that X_1 has a mean value of 6 m/s and follows a Rayleigh distribution truncated at the cut-out wind speed of 25 m/s (u_c in Table 2) since we are interested only in operating wind speed conditions. Also, it is assumed that X_2 (given X_1) has first two moments as described in Fig. 1 and that it follows a lognormal distribution. Details regarding the Hermite model for the response extremes may be obtained from Ronold and Larsen (2000). It should be mentioned that the assumption of the same mean wind speed for the onshore and offshore sites may not strictly be realistic since most offshore sites will in general have mean higher wind speeds. Here, however, the same mean values for both sites are assumed to illustrate the procedures outlined in the following.

Nominal design loads based on 3 load models

1-D Model

In this model, only the ten-minute mean wind speed, X_1, is modeled as random, while the standard deviation of wind speed, X_2, and the ten-minute maximum response, X_3, are held at their (conditional) median levels. Given the reliability index, β, Table 1 may be used to determine the 1-D model nominal load. Based on extremely simple calculations, the 1-, 20-, and 50-year loads at the onshore site were found to be 420.3, 442.3, and 445.2 kN-m, respectively, while the corresponding loads for the offshore site were 390.8, 413.2, and 416.2 kN-m, respectively. Note that randomness in the ten-minute mean wind speed alone was needed to derive these loads. At the two sites, the 1-, 20, and 50-year loads were thus derived based on mean wind speeds of 22.3, 24.5, and 24.8 m/s, respectively. Detailed discussion of the results is only provided for the 2-D and 3-D models in the following since the 1-D model seems overly simplified.

Random Variable	*Distribution*		*Parameters*
X_1 (10-min mean wind speed)	Truncated Rayleigh	$F_{X_1}(x_1) = \dfrac{1-\exp[-(x_1/A)^2]}{1-\exp[-(u_c/A)^2]}$	A=6.77 m/s, u_c=25 m/s (E[X_1]=6.0 m/s)
$X_2\|X_1$ (standard deviation of 10-min wind speed)	Lognormal	$F_{X_2\|X_1}(x_2) = \Phi\left(\dfrac{\ln(x_2)-b_0}{b_1}\right)$ $b_1 = \sqrt{\ln\left(1+\left(\dfrac{\mathrm{D}[X_2 \mid X_1]}{\mathrm{E}[X_2 \mid X_1]}\right)^2\right)}$ $b_0 = \ln\left[\mathrm{E}[X_2 \mid X_1]\right] - \dfrac{1}{2}b_1^2$	<u>*Onshore*</u> E[$X_2\|X_1$] = .0031x_1^2+.0811x_1+.1778 D[$X_2\|X_1$] = -.0004x_1^2+.0122 x_1+.1222 <u>*Offshore*</u> E[$X_2\|X_1$] = .0044x_1^2-.0055x_1+.2934 D[$X_2\|X_1$] = -.0002x_1^2+.0071 x_1+.1365 (using DNV/Risø, 2002; see Fig. 1)
$X_3\|X_1,X_2$ (extreme flap bending moment in 10 minutes)	Hermite model based on four moments	$F_{Y_3}(y_3) = \exp\left[-\nu T \exp\left(-\dfrac{y_3^2}{2}\right)\right]$ $x_3 = x_3(y_3,\mu,\sigma,\alpha_3,\alpha_4)$ based on a transformation that relates the Gaussian extreme, y_3, to the non-Gaussian extreme, x_3 in duration, T (10 min).	$\mu = \mu(x_1)$, $\sigma = \sigma(x_1,x_2)$, and $\nu = \nu(x_1)$ α_3 = -0.0066 α_4 = 2.8174 (see Ronold and Larsen, 2000)

Table 2: Distributions and Parameters for the Random Variables.

2-D Model

Randomness in both of the environmental variables, X_1 and X_2, is now modeled while the load variable, X_3, is still assumed deterministic at its (conditional) median level. Given the reliability index, β, Table 1 may be used to determine the 2-D model nominal load. Using the auxiliary variable, φ, a search may be done over a circle of radius, β, in standard normal space, for the largest value of (median) response. This defines the 2-D nominal load.

As shown in Fig. 2, for a 20-year return period, circles in $\boldsymbol{U}$ space for the two sites map to environmental contours (associated with the target return period) in physical ($\boldsymbol{X}$) space. Parts of these circles are shown as the solid (onshore) and dashed (offshore) curves. The shaded surface represents median response levels for different X_1 and X_2 values. The 20-year maximum values for the onshore and offshore sites are 444.7 and 415.1 kN-m, respectively. The nominal loads for this 2-D model can also be obtained by plotting separate iso-response curves of median values of X_3 together with the 2-D environmental contour in $\boldsymbol{X}$ space and locating the iso-response curve of highest value that is tangent to the 2-D environmental contour.

It should be noted that the environmental contours and the iso-response curves may be constructed independently; hence, these contours are not turbine-specific. The turbine response/load is uncoupled from the environment. The 20-year return period environmental contours for the onshore site (solid curve) and for the offshore site (dashed curve) as well as iso-response curves for the machine are plotted in Fig. 3 from which it may again be confirmed that, at the tangents, the nominal loads are 444.7 kN-m and 415.1 kN-m for the onshore and offshore sites, respectively. Detailed results for all three return periods (1, 20, and 50 years) are summarized in Table 3 (where N refers to the number of ten-minute intervals in the time corresponding to the return period).

3-D Model

Randomness in all three variables, X_1, X_2, and X_3 is now modeled. For a known reliability index, β, one can construct a sphere in standard normal ($\boldsymbol{U}$) space and then perform a search using auxiliary variables, φ and θ, over the sphere of radius, β, as is suggested in Table 1, until the largest value of response, X_3, is obtained. This defines the 3-D nominal load.

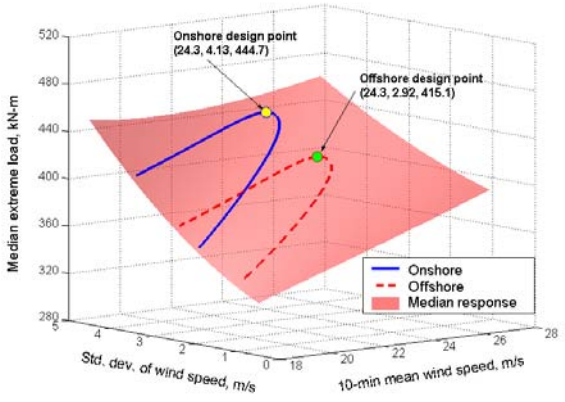

Figure 2: Median Response Surface, 20-year Return Period Onshore and Offshore Environmental Contours, and 2-D Model Design Points.

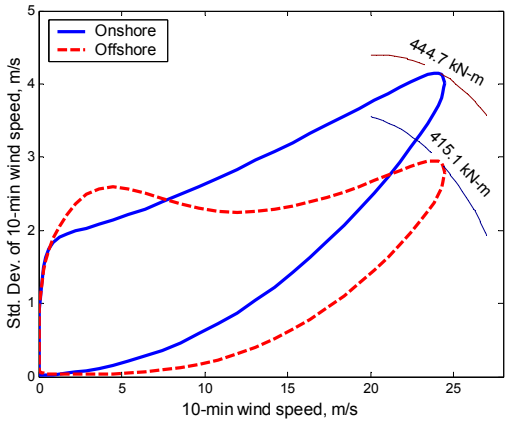

Figure 3: Iso-response Curves and 20-year Return Period Contours for Onshore and Offshore Environments.

Return Period (yrs)	N ($\times 10^3$)	β	Onshore						Offshore					
			2-D			3-D			2-D			3-D		
			X_1 (m/s)	X_2 (m/s)	X_3 (kN-m)	X_1 (m/s)	X_2 (m/s)	X_3 (kN-m)	X_1 (m/s)	X_2 (m/s)	X_3 (kN-m)	X_1 (m/s)	X_2 (m/s)	X_3 (kN-m)
1	49.7	4.12	22.1	3.59	421.9	21.3	3.42	428.7	22.1	2.42	391.8	21.8	2.35	395.8
20	993.6	4.76	24.3	4.13	444.7	23.2	3.84	459.4	24.3	2.92	415.1	23.6	2.72	425.2
50	2484.0	4.95	24.5	4.25	448.8	23.6	3.93	467.8	24.6	3.02	419.1	24.0	2.82	432.8

Table 3: Results summarizing Design Points from the 2-D and 3-D Models for Three Return Periods at the Onshore and Offshore Sites.

As shown in Fig. 4, for a 20-year return period, portions of the spheres in $\boldsymbol{U}$ space for the two sites map to the two surfaces shown for the onshore and offshore sites. The turbine response/load is now coupled with the environments and environmental contours cannot be constructed independently. The 20-year maximum load values for the onshore and offshore sites are 459.4 and 425.2 kN-m, respectively. These are obtained by searching the surfaces of Fig. 4 for the largest value of X_3. Detailed results for all three return periods at the two sites are summarized in Table 3.

Discussion of the 1-D, 2-D, and 3-D model loads

The three models presented above lead to different nominal loads. As is to be expected, the nominal load levels increase with return period. At both sites, it was found that the 1-D and 2-D models yielded very slightly different loads; this is because the variable, X_2, the standard deviation of wind speed, is relatively less important compared to the mean wind speed, X_1. Greater differences are seen when the 3-D model is considered where short-term response uncertainty is included. The 3-D model 20-year loads are about 3-4% higher than the 2-D loads. While for this particular problem, the difference between the 3-D model and the simpler models is small; this may not be the case when response variability (conditional on inflow) is large.

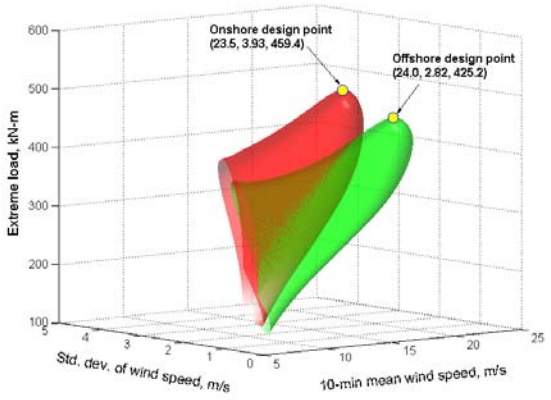

Figure 4: 20-year Return Period Onshore and Offshore Surfaces and 3-D Model Design Point.

Linearized limit state function implications

As was discussed earlier, the Inverse FORM approach is an approximate procedure since it assumes that the limit state function may be linearized at the "design point" and probabilities corresponding to the target return period are associated with this linearized limit state surface, not with the true (generally nonlinear) surface. Thus, there may be errors in the derived nominal load based on the Inverse FORM approach. In the following, we investigate the extent of the error introduced by the linearization assumption by examining the extent to which second-order corrections alter the originally derived loads.

If second-order information of the true limit state function is retained, the first-order probability of failure at the design point may be modified (according to Breitung, 1984) as follows:

$$P_{f,2} \approx \Phi(-\beta) \prod_{i=1}^{n-1} (1+\beta\kappa_i)^{-1/2} \qquad (2)$$

where $P_{f,2}$ is the failure probability including second-order effects and κ_i represents the principal curvatures of the limit state surface in n dimensions at the FORM design point. For the 2-D model (n = 2), there is only one principal curvature that needs to be computed in order to determine $P_{f,2}$. The second-order correction is best explained by studying Fig. 5 where it can be seen that the difference between P_f and $P_{f,2}$ can be thought of graphically as resulting from computing the difference between using, in one case, the points in the unsafe state on one side of the line ($g_I(\boldsymbol{U})$=0) and, in the other, on one side of the quadratic curve ($g_{II}(\boldsymbol{U})$=0). Since the error in this case is conservative (i.e., P_f is greater than $P_{f,2}$), one could correct for this by adjusting the reliability index, β, to a different higher level, β_{equiv}, that is associated with the equivalent dashed line shown in Fig. 5 which is such that the probability of failure associated with it is the same as that associated with the second-order curve, $g_{II}(\boldsymbol{U})$=0. Note that β_{equiv} is easily derived from the principal curvature(s), κ_i, since $\beta_{equiv} = \Phi^{-1}(1-P_{f,2})$. Thus, with the help of an Inverse FORM calculation and computation of local curvatures at the design point, an improved estimate of the design point can be obtained using β_{equiv}. For example, in the 2-D model illustrated in Fig. 5, the new design point in standard normal space is at (u_1^*, u_2^*) obtained using the original design point (u_1, u_2) and the corrected reliability index, β_{equiv}.

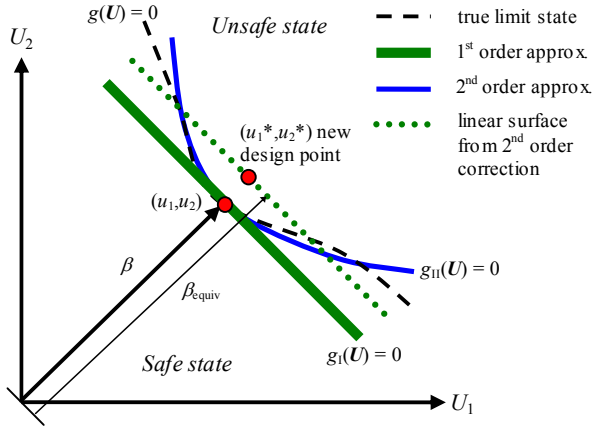

Figure 5: Rationale for Improving the Design Point from the 2-D Model using a Second-order Representation of the Limit State Surface.

To demonstrate the influence of this second-order correction in our nominal load derivation, we consider the 2-D model results for the onshore site that were presented before. Because our limit state function is not available in analytical closed form, the single principal curvature (related to the second derivative of the limit state function, $g(\boldsymbol{U})$) needed at the 2-D model design point in standard normal space was determined numerically using a central-difference scheme with error on the order of Δu^6 where Δu is the step size which was taken to be 0.01 (see e.g. Al-Khafaji and Tooley, 1986). For the 1-year return period case shown in Fig. 6(a), the limit state function is slightly concave inwards (towards the origin) and hence β_{equiv} is smaller than β (see Fig. 7) and the corrected load is slightly smaller too. For the 20- and 50-year return periods where the limit state is concave outwards (away from the origin) as can be seen in Figs. 6(b) and 6(c), the situation is such that β_{equiv} is larger than β (see Fig. 7) and the corrected loads are larger than were found from the Inverse FORM calculations. From Fig. 7, it may be noted that the difference between the reliability index values, β and β_{equiv}, is not significant at any return period for the onshore site. Similar results were obtained for the offshore site. The curvature at the design point was greater at higher return periods (see Fig. 6(c)) and this leads to the greatest differences between β and β_{equiv} for the 50-year return period case, for example. Table 4 summarizes the derived loads based on second-order corrections for the onshore site. Comparing the results in Table 4 with those of the 2-D model in Table 3, we observe negligibly small differences between the design loads in the two cases.

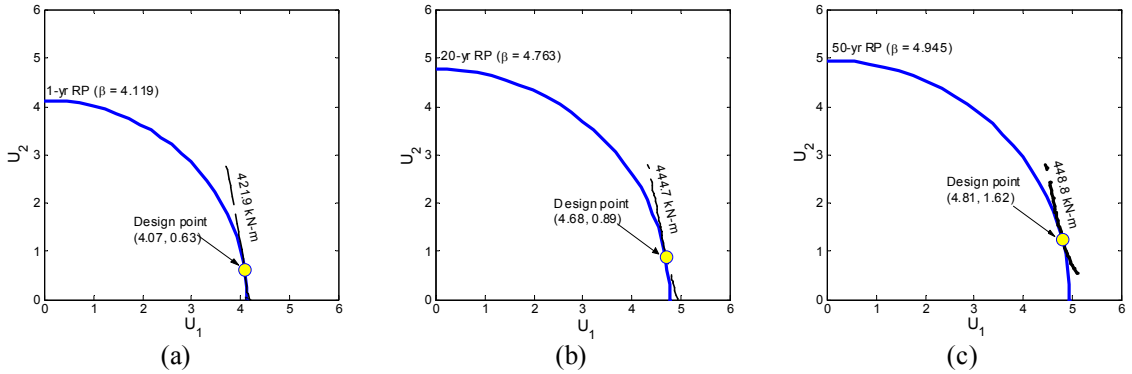

Figure 6: *T*-year Return Period Onshore Environmental Contour and Iso-response Curves at 2-D Design Points in Standard Normal (*U*) Space – (a) *T* = 1 yr., (b) *T* = 20 yrs., (c) *T* = 50 yrs.

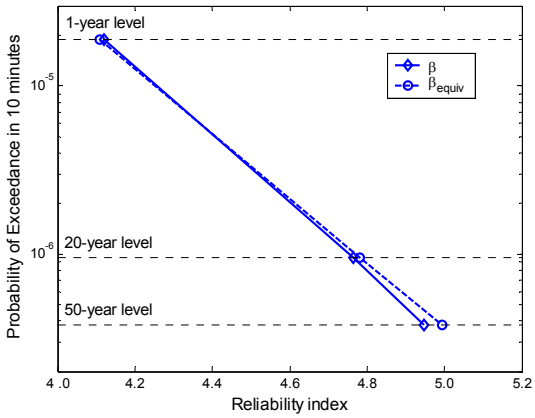

Figure 7: Reliability Indices for Different Return Periods at the Onshore Site showing the Effect of a Second-order Representation of Limit State Function in the 2-D Model.

Based on the above findings, we conclude that at least for the illustrations considered here, the Inverse FORM procedure, where the limit state function is assumed linear, yields design loads that have very small error due to the linearization. However, since this conclusion is case-specific, it may be prudent to evaluate the influence of second-order characteristics of the limit state surface by employing the simple procedure provided in this section.

Response Variability Implications

Based on the various results presented thus far, it is believed that the largest source of error in deriving design loads arises when response variability is neglected (as is done in the 1-D and 2-D models). To minimize this error, a complete joint probability distribution of the three random variables is required, as is achieved with the 3-D model. The 2-D model, however, is of special interest because it uncouples the environment from the response. This is especially convenient when considering the same turbine at different sites (as is done here) as well as when considering alternative turbines for a specified environment.

Return Period (yrs)	β_{equiv}	2-D (with second-order correction)		
		X_1 (m/s)	X_2 (m/s)	X_3 (kN-m)
1	4.11	22.0	3.58	421.5
20	4.78	24.2	4.16	445.2
50	4.99	24.5	4.29	449.8

Table 4: Results summarizing Design Points based on a Local Second-order Correction with the 2-D Model for Three Return Periods (Onshore Environment).

The 2-D model's limitation (relative to the 3-D model) is that it employs the median value of X_3 conditional on X_1 and X_2 to arrive at nominal design load levels. If appropriately derived fractiles for X_3 (other than the median) can be obtained that account for response variability even approximately, the advantages of the 2-D model (namely uncoupled environment and turbine) may be retained and more accurate loads derived. One approach to arrive at the appropriate fractile for X_3 is to employ omission sensitivity factors (see Madsen, 1988). A "Modified 2-D Model" is introduced using this approach. The desired fractile, p_3, for the response variable is obtained in terms of the direction cosine, α_3, of the limit state function in the direction of the standard normal variable, U_3 and at the 2-D model design point.

$$p_3 = \Phi\left(\left(1-\sqrt{1-\alpha_3^2}\right)\beta/\alpha_3\right); \quad X_3^+ = F^{-1}_{X_3|X_1,X_2}(p_3) \qquad (3)$$

where X_3^+ as given in Eq. (3) may be used instead of the value of X_3 shown for the 2-D model in Table 1. It should be noted that α_3 is a measure of the importance of the response random variable. A higher value of α_3 will yield fractiles farther away from the median; it is computed using gradients of the limit state function at the 2-D model design point in standard normal space.

$$\alpha_3 = \frac{\partial g(\mathbf{u})/\partial u_3}{\| \nabla g(\mathbf{u}) \|} \qquad (4)$$

Thus, the required fractile, p_3, may be determined with a few additional calculations following a 2-D model analysis. Here, gradients of the limit state function were determined numerically by employing a central-difference scheme with error on the order of Δu^6 where Δu is the step size which was taken to be 0.01. Figure 8 summarizes the onshore site results from the 1-D, 2-D, and 3-D models as well as results obtained using second-order corrections of the limit state function to the 2-D model and results from the Modified 2-D model based on Eqs. 3 and 4. The nominal bending loads from the Modified 2-D model are very similar to those from the 3-D model indicating that if response variability is accounted for even approximately using the approach outlined (and summarized in Eqs. 3 and 4), the accuracy in design loads is improved and the advantages of the 2-D model are preserved. For the offshore site as well, this improvement was observed as is evident from Table 5 which summarizes results for both sites using the Modified 2-D model. The direction cosines, α_3, are included in the table as well as the modified fractile levels, p_3. The nominal loads may be compared with the 3-D model loads in Table 3 to verify the accuracy of the proposed Modified 2-D procedure. It should be noted that the fractile levels required get farther away from the median as the return period increases. Also, at the onshore site, response variability is slightly more important than at the offshore site.

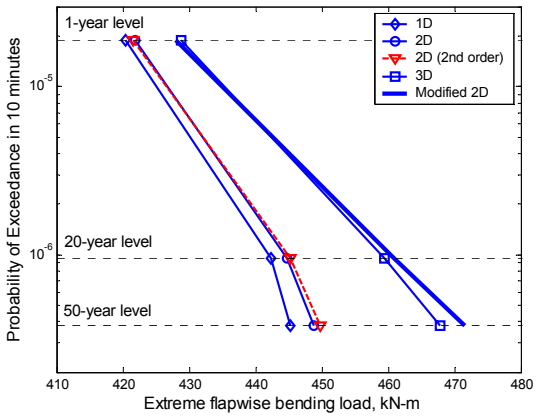

Figure 8: Extreme Flapwise Bending Moment for 1-, 20-, and 50-year Return Periods based on Various Models for the Onshore Site.

CONCLUSIONS

We have presented a procedure to establish nominal loads for the design of wind turbines against ultimate limit states at two distinct sites – one onshore, the other offshore. Various alternative load models were compared. An inverse reliability approach was employed to estimate the design loads for three different return periods. For the 600kW wind turbine considered, extreme flapwise bending loads were studied and it was found that the difference between the nominal loads derived from 1-D and 2-D models was small since the standard deviation of wind speed at the hub height had a very small effect on the extreme bending load compared with the mean wind speed. Including uncertainty in the short-term maximum bending load conditional on inflow (in the 3-D model) caused somewhat higher loads than in the 1-D and 2-D models.

Two issues related to accuracy of the Inverse FORM predictions were studied. It was determined that the implied use of a linearized limit state function does not lead to significant error in derived loads; this was

Return Period (yrs)	Onshore			Offshore		
	Direction cosine, α_3	Modified fractile for X_3	X_3 (kN-m)	Direction cosine, α_3	Modified fractile for X_3	X_3 (kN-m)
1	0.25	0.70	428.0	0.20	0.66	395.5
20	0.45	0.87	460.9	0.37	0.82	425.5
50	0.55	0.93	471.6	0.51	0.91	435.8

Table 5: Results from Modified 2-D Model for Three Return Periods.

verified by making second-order corrections using curvatures of the limit state surface. Neglecting response variability, on the other hand, was found to lead to greater error (as manifested by differences in loads derived based on 2-D and 3-D models). A Modified 2-D model was proposed and demonstrated to yield almost similar nominal loads as were obtained with the 3-D model as long as suitably derived "higher-than-median" fractiles for the response variable were obtained first by using some additional computations of gradients of the limit state surface at the 2-D model design point. The attractiveness of the Modified 2-D model is not only the improved accuracy but the fact that the environment and turbine response are uncoupled. Implications of this are that when the same turbine is considered for different sites, only the site-specific inflow variability needs to be correctly represented. Similarly, if at a given site, two alternative designs are being considered, only the machine-specific response variability (conditional on inflow) needs to be available from simulation studies or measurements and this can be combined with the site's inflow characterization in the 2-D or Modified 2-D approach in order to derive appropriate design loads.

ACKNOWLEDGEMENTS

The authors gratefully acknowledge the financial support provided by Grant No. 003658-0272-2001 awarded through the Advanced Research Program of the Texas Higher Education Coordinating Board. They also acknowledge additional support from Sandia National Laboratories by way of Grant No. 30914.

REFERENCES

1. Al-Khafaji, A. W. and Tooley J. R. (1986). *Numerical Methods in Engineering Practice*, Holt, Rinehart and Winston Inc., New York, USA.
2. Breitung, K. (1984). *Asymptotic Approximations for Multinormal Integrals*, Journal of Engineering Mechanics, ASCE, Vol. 110, No. 3, pp. 357-366.
3. DNV/Risø (2002). *Guidelines for Design of Wind Turbines*, ed. 2, Det Norske Veritas, Copenhagen and Risø National Laboratory.
4. Fitzwater, L. M., Cornell, C. A., and Veers, P. S. (2003). *Using Environmental Contours to Predict Extreme Events on Wind Turbines*, Wind Energy Symposium, AIAA/ASME, Reno, Nevada, pp. 244-258.
5. IEC/TC88 61400-1 ed. 2 (1998). *Wind turbine generator systems-part 1: Safety Requirements*, International Electrotechnical Commission (IEC).
6. Li, H. and Foschi, R. O. (1998). *An Inverse Reliability Method and its Application*, Structural Safety, Vol. 20, pp. 257-270.
7. Madsen, H. O. (1988). *Omission Sensitivity Factors*, Structural Safety, Vol. 5, pp. 35-45.
8. Ronold, K. O. and Larsen G. C. (2000). *Reliability-based Design of Wind-turbine Rotor Blades against Failure in Ultimate Loading*, Engineering Structures, Vol. 22, pp. 565-574.
9. Rosenblatt, M. (1952). *Remarks on a Multivariate Transformation*, Ann. Math. Stat., Vol. 23, pp. 470-472.
10. Saranyasoontorn, K. and Manuel, L. (2003). *Efficient models for wind turbine extreme loads using inverse reliability*, Proceedings of the Response of Structures to Extreme Loading Conference, Toronto, Canada.
11. Winterstein, S. R., Ude, T. C., Cornell, C. A., Bjerager, P., and Haver, S. (1993). *Environmental Contours for Extreme Response: Inverse FORM with Omission Factors*, Proc. ICOSSAR-93, Innsbruck.